JAST
Journal of Aerospace Science and Technology

Pages: 38-49 / Vol. 16/ No. 2 /Summer- Fall 2023

Journal of Aerospace Science and Technology

www:jast.ias.ir

Scienctifie-Research Article

New Guidance Method for High Altitude Target Based on Constrained Incremental Predictive Control

Mohammad Yavari[1], **Nemat Allah Ghahramani**[2]*, **Reza Zardashti**[3], **Jalal Karimi**[4]
1-3-4- Faculty of Aerospace Engineering , Malek Ashtar University, Tehran, Iran
2- Faculty of Electrical and Coumputer Engineering ,Malek Ashtar University, Tehran, Iran

Keywords: *guidance, parallel navigation, constrained incremental predictive control, high speed and high altitude target*

ABSTRACT

In this paper, a new midcourse guidance algorithm for intercepting high-altitude targets is proposed. A part of the target flight path is outside the atmosphere. The maximum acceleration command is designed as a variable constraint that varies with altitude. This physical limitation is happened for the aerodynamically control interceptors at high altitudes because of decreasing air density. Based on a generalized incremental predictive control approach, a new formulation for parallel navigation guidance law is proposed. Using the nonlinear kinematic equations of the target-interceptor, the commands of the new guidance method are computed by optimization of a cost function involving the velocity perpendicular to the line of sight errors and guidance commands. An important feature of the proposed method is the minimization of the line-of-sight angular rate in a finite period of time. The various simulation results of the proposed guidance law show the higher effectiveness of the designed guidance law in comparison with proportional navigation and sliding mode guidance.

Introduction

Intercepting high-altitude targets in which a part of their flight trajectory is outside of the atmosphere is among the essential issues in today's defence research. The most significant problems are the higher speed of targets relative to the interceptors and the high altitude of the engagement [1, 2]. For these situations, two groups of scenarios are proposed:

In the first (Fig. 1), the engagement is head-on [3]. In this way, the interceptor approaches the target with an angle between their velocities that covers 90 to 180 degrees. In the second, the interceptor is in front of the target, and both move in the same direction [4-6]. In this scenario, the interceptor's velocity is considered lower than the target velocity, and therefore, the target hits the interceptor from behind. In this engagement the relative closing velocity is decreased (Fig. 2).

1 PhD. Candidate
2 Associate Professor (Corresponding Author), **Email:** Ghahremani@mut.ac.ir
3 Associate Professor
4 Associate Professor

DOI : 10.22034/jast.2023.383679.1143
Submit: 29-01-2023 / Accepted: 06-06-2023
Print ISSN:1735-2134 Online ISSN: 2345-3648

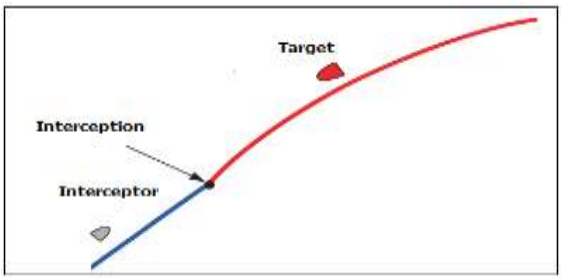

Fig .1 Head-on engagement.

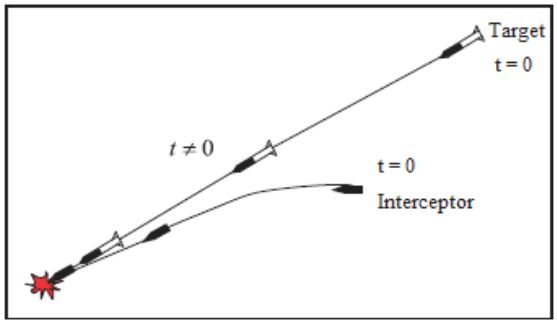

Fig. 2 Head-pursuit engagement [5].

Various guidance methods for these interceptors have been developed. Some of them are based on non-linear control methods, such as sliding mode. Shima and Gulan [7] presented a guidance law based on the idea of parallel navigation and sliding mode theory, where the sliding surface is selected proportional to the line-of-sight (LOS) rate. Lee et al. [8] used the sliding mode control to design a guidance law with a specific capture region and finite time convergence. Sun et al. [9] proposed a guidance method with the capablity of adjusting desired impact angle using the back-stepping method.

Optimal control methods are also used for designing guidance laws. Chen et al. [10] used the optimal control optimizing fuel consumption cost function. In the method proposed by Ryu et al. [11], the time-to-go is considered in the cost function, and the guidance command exponentially is decreased versus time-to-go. Lee et al. [12] studied the efficiency of a guidance law designed based on differential geometry against high-velocity targets using the Lyapunov Method. Jung et al. [13] has presented a guidance law based on the change of the velocity magnitude. This method consumes less fuel compared to the true proportional guidance method. Kim et al. [14] proposed a guidance method to minimize energy consumption using the feedback linearization method.

Among the novel methods of designing and performing the guidance process, the reinforcement learning [15] approach can be enumerated. In this method, after learning the guidance system, the line-of-sight angle and its change rate are mapped directly to guidance commands by the learning system without using guidance law. Gaudet et al. [16] was designed to integrate a guidance and control system for moving targets using a reinforced learning approach.

In recent years, the predictive control strategy has been used to solve control problems. This method is based on the optimal solution in a finite time.

The predictive control command is calculated using the system model to optimize the defined cost function during a limited time window named prediction horizon [17]. The significant capability of this method is the possibility of applying constraints on the system states [18]. In this method, an optimization problem must be solved at each step time. Today, With advanced technologies on microprocessors this control method has been widely used [19-22]. Kung et al. [23] proposed an algorithm to plan a salvo attack against a stationary target using predictive control. Bachtiar et al. [24] proposed an integrated guidance and control approach for interceptors using non-linear predictive control. Wang and Hei [25] used the sliding mode theory and predictive control to design the guidance law.

Generalized predictive control is one of the most applicable predictive control algorithms. A type of this family is the generalized incremental predictive control algorithm [26]. In this method the increment states are used in the model and the incremental form is performed.

Comparing this method with the generalized predictive control method shows that the GIPC has a higher robustness with respect to uncertainties and disturbances.

The purpose of this paper is to present the midcourse guidance method for high-altitude targets interception. Since the increase in flight height decreases the aerodynamic forces and moments, the guidance time in the midcourse phase with aerodynamic control is finite. In addition, the guidance commands which executed by aerodynamic forces and moments must also be decreased. Therefore, the limit of the maximum guidance command should be a function of height in the process of guidance command generation.

This paper presents a new guidance method based on an incremental predictive control approach.

The innovation of this method is introducing the incremental state-space model for guidance equations and then, defining a constrained cost function in order to optimize guidance commands using predictive control ideas in a limited time cycle.

The advantage of this new method over other guidance approaches is zeroing the line-of-sight angular rate and compensating for the guidance error in a shorter time. Note that this interesting feature is very important. Moreover, in this new method, the maximum lateral acceleration executable by the interceptor, which varies with height, has been considered as a constraint in the cost function in order to generate the guidance commands. This variable constraint in the presented method is considered as a fixed saturation in other references. Simulations of different scenarios for interceptor's flight show that this method is more accurate and efficient.

The remainder of this paper is organized as follows. In section two, kinematic equations are described. Section three discusses calculating the constraint control command using predictive increment control. In section four, first, the extracted system models and then the designed algorithm is presented. In section five, resents some numerical results and validates the effectiveness of the approach. Finally, conclusions are given in section six.

Kinematic Equations of the Target–Interceptor

The planar interception geometry is depicted in Fig. 3. The corresponding nonlinear kinematics are given by [27]:

$$\dot{R} = V_R \tag{1}$$

$$\dot{\lambda} = \frac{V_\lambda}{R} \tag{2}$$

$$\dot{\gamma}_M = \frac{a_M}{V_M} \tag{3}$$

$$\dot{\gamma}_T = \frac{a_T}{V_T} \tag{4}$$

$$\dot{V}_R = \frac{V_\lambda^2}{R} + a_\mathrm{T}\sin(\lambda - \gamma_\mathrm{T}) - a_\mathrm{M}\sin(\lambda - \gamma_\mathrm{M}) \tag{5}$$

$$\dot{V}_\lambda = \frac{-V_R V_\lambda}{R} + a_T\cos(\lambda - \gamma_T) - a_M\cos(\lambda - \gamma_M)) \tag{6}$$

where R is the relative range, λ is the line-of-sight angle, V_M and V_T are the velocity of the interceptor and the target, respectively. γ_M and γ_T are the flight-path angles of the interceptor and target, respectively. α_M and α_T are interceptors and target acceleration, respectively. V_R is the relative velocity along the line-of-sight and V_λ is the relative velocity perpendicular to the line-of-sight.

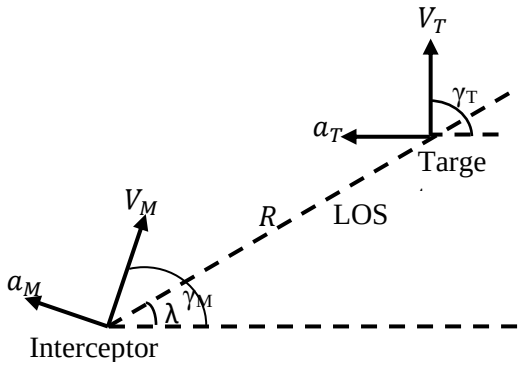

Fig. 3 Engagement geometry

Constrained Incremental Predictive Control method

The linear state-space model of a discrete-time system has the following general form:

$$\boldsymbol{x}(k+1) = \boldsymbol{A}\boldsymbol{x}(k) + \boldsymbol{B}\boldsymbol{u}(k) \tag{7}$$

$$y(k+1) = \boldsymbol{C}\boldsymbol{x}(k+1) \tag{8}$$

where $\boldsymbol{A} \in \boldsymbol{R}^{n*n}$, $\boldsymbol{B} \in \boldsymbol{R}^n$, and $\boldsymbol{C} \in \boldsymbol{R}^n$ are the matrices of state-space, $\boldsymbol{x} \in R^n$ states, $\boldsymbol{u} \in R^n$ control input, and $y \in$ R output of the system. n_u is the control horizon and n_y is the prediction horizon. The state-space differential equation is written as follows:

$$\Delta\boldsymbol{x}(k+1) = \boldsymbol{A}\,\Delta\boldsymbol{x}(k) + \boldsymbol{B}\,\Delta\boldsymbol{u}(k) \tag{9}$$

The state-space model is used to predict output in the future horizon. system-state space at time $k+n_y$ is needed to predict the ouput in the future horizon n_y. If the states at time k are available, they can be predicted at time $k+n_y$ [26]. Output prediction is as follows:

$$\vec{\boldsymbol{y}}_k = \boldsymbol{p}_{y0}\boldsymbol{x}(k) - \boldsymbol{p}_{y1}\boldsymbol{x}(k-1) + \boldsymbol{H}_y\Delta\vec{\boldsymbol{u}}_{k-1} \tag{10}$$

Where $\vec{\mathbf{y}}_\mathrm{k}$ is the system's predictive output vector and $\Delta\vec{\boldsymbol{u}}_{\mathrm{k}-1}$ is the input vector

$$\vec{\boldsymbol{y}}_k = \begin{bmatrix} y(k+1) \\ y(k+2) \\ \cdot \\ \cdot \\ y(k+N_y) \end{bmatrix} \tag{11}$$

$$\Delta\vec{\boldsymbol{u}}_{k-1} = \begin{bmatrix} \Delta u(k) \\ \Delta u(k+1) \\ \cdot \\ \cdot \\ \Delta u(k+n_u-1) \end{bmatrix} \quad (12)$$

$$\boldsymbol{P}_{y0} = \begin{bmatrix} C(A+I) \\ C(A^2+A+I) \\ \cdots \\ C(A^{N_y}+\cdots+A+I) \end{bmatrix} \quad (13)$$

$$\boldsymbol{P}_{y1} = \begin{bmatrix} C(A) \\ C(A^2+A) \\ \cdots \\ C(A^{N_y}+\cdots+A) \end{bmatrix} \quad (14)$$

$$\boldsymbol{H}_y = \begin{bmatrix} CB & 0 & \cdots & 0 \\ C(A+I)B & CB & \cdots & 0 \\ \vdots & & \ddots & \vdots \\ C\left(\sum_{i=0}^{n_y-1} A^i\right)B & \cdots & & C\left(\sum_{i=0}^{n_y-n_u} A^i\right)B \end{bmatrix} \quad (15)$$

The control command is calculated in predictive control by minimizing the predictive output deviation from the reference signal and the minimum control effort. It is performed by defining and minimizing the following cost function.

$$J = (\boldsymbol{Y}_k - \boldsymbol{Y}_R)^T \boldsymbol{R}_y (\boldsymbol{Y}_k - \boldsymbol{Y}_R) + \Delta \boldsymbol{U}_{K-1}{}^T \boldsymbol{R}_u \Delta \boldsymbol{U}_{K-1} \quad (16)$$

Where $\boldsymbol{Y}_R$ is the future desired output vector, $\boldsymbol{Y}_K$ is the predictive output vector, $\Delta\boldsymbol{U}$ is the incremental input command, $\boldsymbol{R}_y$ is the positive semidefinite output weight matrix, and $\boldsymbol{R}_u$ is the positive-definite input weight matrix. If there exist some constraints in the system model, they should be considered in the cost function minimization. The input constraints can be expressed by [28]:

$$\boldsymbol{M}\Delta\boldsymbol{u}_{k-1} \leq \boldsymbol{N} \quad (17)$$

$$\boldsymbol{M} = \begin{bmatrix} \boldsymbol{T} \\ -\boldsymbol{T} \\ \boldsymbol{I} \\ -\boldsymbol{I} \end{bmatrix}, \quad N = \begin{bmatrix} \vec{1}\boldsymbol{u}_{max} - \boldsymbol{u}(k-1)\vec{1} \\ \vec{1}\boldsymbol{u}_{max} - \boldsymbol{u}(k-1)\vec{1} \\ \overrightarrow{1d}\boldsymbol{u}_{max} \\ \overrightarrow{1d}\boldsymbol{u}_{max} \end{bmatrix} \quad (18)$$

Where $\boldsymbol{T}$ is an n_u*n_u lower triangular matrix whose entries are ones, and $\vec{1}$ is an n_u vector, whose entries are ones. The control signal is obtained from equation (19).

$$\Delta\boldsymbol{U} = \boldsymbol{K}_{GIPC}\left(\boldsymbol{H}_y^T\boldsymbol{R}_y(\boldsymbol{R} - \boldsymbol{P}_{y0}\boldsymbol{x}(k) + \boldsymbol{p}_{y1}\boldsymbol{x}(k-1) - \boldsymbol{M}^T\lambda^*)\right) \quad (19)$$

$$\boldsymbol{K}_{GIPC} = \left(\boldsymbol{R}_u + \boldsymbol{H}_y^T\boldsymbol{R}_y\boldsymbol{H}_y\right)^{-1} \quad (20)$$

The optimal Lagrange multipliers λ* is calculated using Quadratic Programming.

Design of Guidance Algorithm Using the Constrained Incremental Predictive Control Method

In the present study, the guidance algorithm for an interceptor with height-varying acceleration constraint is presented. this algorithm is implemented based on the parallel navigation idea (nullify the line-of-sight rate) and using the constrained incremental predictive control method.

Discretization of Motion Equations

State variables of the motion equations are as follows:

$$\boldsymbol{x} = [R, V_R, \lambda, V_\lambda, \gamma_M] \quad (21)$$

According to equations (1)-(6) and (21) the system can be formulated as:

$$\dot{x}_1 = x_2 \quad (22)$$

$$\dot{x}_2 = \frac{x_4^2(t)}{x_1(t)} - \sin(x_3(t) - x_5(t))u + a_T\sin(\lambda - \gamma_T) \quad (23)$$

$$\dot{x}_3 = \frac{x_4(t)}{x_1(k)} \quad (24)$$

$$\dot{x}_4 = -\frac{x_2(t)x_4(t)}{x_1(t)} - \cos(x_3(t) - x_5(t)x)u + a_T\cos(\lambda - \gamma_T) \quad (25)$$

$$\dot{x}_5 = \frac{u}{\mathrm{V_M}} \quad (26)$$

To design the guidance method based on constrained incremental predictive control method, state equations of the system should be modeled in discrete time form. Discretization is performed using the Euler Method. Assuming that the target is without maneuver, the target acceleration is ignored here.

$$x_1(k+1) = x_1(k) + dt(x_2(k)) \tag{27}$$

$$\begin{aligned} x_2(k+1) = x_2(k) \\ + dt\left(\frac{x_4^2(k)}{x_1(k)}\right. \\ - \sin(x_3(k) \\ \left. - x_5(k))u\right) \end{aligned} \tag{28}$$

$$x_3(k+1) = x_3(k) + dt\left(\frac{x_4(k)}{x_1(k)}\right) \tag{29}$$

$$\begin{aligned} x_4(k+1) = x_4(k) \\ + dt\left(-\frac{x_2(k)x_4(k)}{x_1(k)}\right. \\ - \cos(x_3(k) \\ \left. - x_5(k)x)u\right) \end{aligned} \tag{30}$$

$$x_5(k+1) = x_5(k) + dt\left(\frac{1}{V_M}u\right) \tag{31}$$

where dt is the time of discretization and has vaue of 10 milliseconds. As seen, the equations of the system are non-linear and should become linear. The linearized equations after the linearization process are as follows:

$$\boldsymbol{x}(k+1) = \boldsymbol{x}(k) + dtf(\boldsymbol{x}(k), \boldsymbol{u}(k)) \tag{32}$$

$$\begin{aligned} \Delta\boldsymbol{x}(k+1) = \Delta\boldsymbol{x}(k) + dt\frac{\partial f}{\partial x}\Delta\boldsymbol{x}(k) \\ + dt\frac{\partial f}{\partial u}\Delta\boldsymbol{u} \end{aligned} \tag{33}$$

$$\begin{aligned} \Delta\boldsymbol{x}(k+1) = (I + dt\frac{\partial f}{\partial x})\Delta\boldsymbol{x}(k) \\ + dt\frac{\partial f}{\partial u}\Delta\boldsymbol{u} \end{aligned} \tag{34}$$

$$\frac{\partial f}{\partial x} = \begin{bmatrix} 0 & 1 & 0 \\ -\frac{x_4^2}{x_1^2} & 0 & -u\cos(x_3 - x_5) \\ -\frac{x_4}{x_1^2} & 0 & 0 \\ \frac{x_2 x_4}{x_1^2} & -\frac{x_4}{x_1} & u\sin(x_3 - x_5) \\ 0 & 0 & 0 \end{bmatrix} \quad \ldots$$

$$\begin{bmatrix} 0 & 0 \\ 2\frac{x_4}{x_1} & u\cos(x_3 - x_5) \\ \frac{1}{x_1} & 0 \\ -\frac{x_2}{x_1} & -u\sin(x_3 - x_5) \\ 0 & 0 \end{bmatrix} \tag{35}$$

$$\frac{\partial f}{\partial u} = \begin{bmatrix} 0 \\ -\sin(x_3 - x_5) \\ 0 \\ -\cos(x_3 - x_5) \\ \frac{1}{V_m} \end{bmatrix} \tag{36}$$

Stability Analysis

In this section, sufficient conditions for the asymptotic stability of the proposed method are described. Assume that at current sample time k, the future of the control trajectory $\Delta\boldsymbol{u}_{k+i|k}, i = 0,1,\ldots,n-1$ is optimized by minimizing the cost function:

$$\begin{aligned} \boldsymbol{J} \\ = \sum_{\boldsymbol{i=1}}^{\boldsymbol{n}} (\boldsymbol{y}_{\boldsymbol{k+i|k}} - \boldsymbol{y}^{\boldsymbol{r}}_{\boldsymbol{k+i|k}})^{\boldsymbol{T}} \boldsymbol{R}_{\boldsymbol{y}}(\boldsymbol{y}_{\boldsymbol{k+i|k}} \\ - \boldsymbol{y}^{\boldsymbol{r}}_{\boldsymbol{k+i|k}}) \\ + \sum_{\boldsymbol{i=0}}^{\boldsymbol{n-1}} (\Delta\boldsymbol{u}_{\boldsymbol{k+i}})^{\boldsymbol{T}} \boldsymbol{R}_{\boldsymbol{u}}(\Delta\boldsymbol{u}_{\boldsymbol{k+i}}) \end{aligned} \tag{37}$$

As a result of zeroing reference, the cost function can be simplified as

$$\begin{aligned} \boldsymbol{J} \\ = \sum_{\boldsymbol{i=1}}^{\boldsymbol{n}} (\boldsymbol{y}_{\boldsymbol{k+i|k}})^{\boldsymbol{T}} \boldsymbol{R}_{\boldsymbol{y}}(\boldsymbol{y}_{\boldsymbol{k+i|k}}) \\ + \sum_{\boldsymbol{i=0}}^{\boldsymbol{n-1}} (\Delta\boldsymbol{u}_{\boldsymbol{k+i}})^{\boldsymbol{T}} \boldsymbol{R}_{\boldsymbol{u}}(\Delta\boldsymbol{u}_{\boldsymbol{k+i}}) \end{aligned} \tag{38}$$

After calculate future input $\Delta\boldsymbol{U}_k$, Only the first sample $\Delta\boldsymbol{u}_k$is implemented. Closed-loop stability is based on a constraint, which is $y_{k+n|k=0}$. Algorithm stability is summarized in the following theorem. This theorem and assumptions are described in [28, 29]

Theorem - Consider the cost function (38) and assume that

1- Constraint is specified as $y_{k+n|k} = 0$ where $y_{k+n|k}$ is the terminal output resulting from the control sequence $\Delta\boldsymbol{u}_{k+i-1}$, $i = 1,2,\ldots,n$.
2- for each sampling instant k there exists a solution $\Delta\boldsymbol{u}_k$ such that the cost function *J* is

minimized subject to the equality constraint $y_{k+n|k=0}$.

Subject to the assumptions, the closed-loop model predictive control system is stable.

Proof. The key to the stability result is to choose the cost function (38) as the Lyapunov function

$$\begin{aligned} &\boldsymbol{v(x(k),k)} \\ &= \sum_{\boldsymbol{i=1}}^{\boldsymbol{n}} (\boldsymbol{y_{k+i|k}})^{\boldsymbol{T}}\, \boldsymbol{R_y} (\boldsymbol{y_{k+i|k}}) \\ &+ \sum_{\boldsymbol{i=0}}^{\boldsymbol{n-1}} (\boldsymbol{\Delta u_{k+i}})^{\boldsymbol{T}}\, \boldsymbol{R_u} (\boldsymbol{\Delta u_{k+i}}) \end{aligned} \quad (39)$$

It is seen that $v(x(k),k)$ is positive definite. At time *k+1*, the Lyapunov function becomes:

$$\begin{aligned} &\boldsymbol{v(x(k+1),k+1)} \\ &= \sum_{\boldsymbol{i=1}}^{\boldsymbol{n}} (\boldsymbol{y_{k+1+i|k+1}})^{\boldsymbol{T}}\, \boldsymbol{R_y} (\boldsymbol{y_{k+1+i|k+1}}) \\ &+ \sum_{\boldsymbol{i=0}}^{\boldsymbol{n-1}} (\boldsymbol{\Delta u_{k+1+i}})^{\boldsymbol{T}}\, \boldsymbol{R_u} (\boldsymbol{\Delta u_{k+1+i}}) \end{aligned} \quad (40)$$

We need to make a link between the Lyapunov function at sample time *k + 1* and the function at sample time *k*. For each sample time obtaining the optimal input command sequence, $\Delta\bar{\boldsymbol{U}}_{(k+1)}$ define as follow: $\Delta\bar{\boldsymbol{U}}_{(k+1)}$ is input command sequence at time k+1 which predict in time k and the final state is replaced with zero.

$$\Delta\bar{\boldsymbol{U}}_{(k+1)} = \begin{Bmatrix} \Delta\boldsymbol{u}_{(k+1|k)}, \Delta\boldsymbol{u}_{(k+2|k)}, \cdots, \\ \Delta\boldsymbol{u}_{(k+n-1|k)}, 0 \end{Bmatrix} \quad (41)$$

Because of optimality in the solution of ΔU_{k+1}, it is seen that:

$$\begin{aligned} &\boldsymbol{v(x(k+1),k+1)} \\ &\leq \bar{\boldsymbol{v}}\boldsymbol{(x(k+1),k+1)} \end{aligned} \quad (42)$$

where $\bar{v}(\boldsymbol{x}(k+1),k+1)$ is similar to (40) except that the control sequence is replaced by the feasible sequence $\Delta\bar{\boldsymbol{U}}_{(k+1)}$.

$$\begin{aligned} &\boldsymbol{v(x(k+1),k+1)} - \boldsymbol{v(x(k),k)} \\ &\leq \bar{\boldsymbol{v}}\boldsymbol{(x(k+1),k+1)} \\ &- \boldsymbol{v(x(k),k)} \end{aligned} \quad (43)$$

Note that because the $\bar{v}(\boldsymbol{x}(k+1),k+1)$ and $v(\boldsymbol{x}(k),k)$ shares the same control sequence and the same state sequence for the sample time $k+1,k+2,\ldots,k+n-1$, the difference between these two functions is

$$\begin{aligned} &\bar{\boldsymbol{v}}\boldsymbol{(x(k+1),k+1)} - \boldsymbol{v(x(k),k)} \\ &= \boldsymbol{\left(y_{k+n|k}\right)^T R_y \left(y_{k+n|k}\right)} \\ &- \boldsymbol{\left(y_{k+1|k}\right)^T R_y \left(y_{k+1|k}\right)} \\ &- \boldsymbol{(\Delta u_k)^T R_u (\Delta u_k)} \end{aligned} \quad (44)$$

From the first assumption, we have

$$\begin{aligned} &\bar{\boldsymbol{v}}\boldsymbol{(x(k+1),k+1)} - \boldsymbol{v(x(k),k)} \\ &= -\boldsymbol{\left(y_{k+1|k}\right)^T R_y \left(y_{k+1|k}\right)} \\ &- \boldsymbol{(\Delta u_k)^T R_u (\Delta u_k)} \end{aligned} \quad (45)$$

Hence, the difference of the Lyapunov function is

$$\begin{aligned} &\boldsymbol{v(x(k+1),k+1)} - \boldsymbol{v(x(k),k)} \\ &\leq -\boldsymbol{\left(y_{k+1|k}\right)^T R_y \left(y_{k+1|k}\right)} \\ &- \boldsymbol{(\Delta u_k)^T R_u (\Delta u_k)} < \boldsymbol{0} \end{aligned} \quad (46)$$

which we see is negative. Hence, we have established the asymptotic stability of the proposed algorithm.

Simulation Results

To intercept the target, the rate of the line-of-sight rotation, or in other words, the relative velocity perpendicular to the line-of-sight, should be zero according to the parallel navigation idea. V_λ is considered the system output, according to the system equations (22-26). Therefore, the future desired output vector $\boldsymbol{Y}_{\mathrm{R}}$, must be zero. The acceleration command generated by the predictive guidance causes V_λ to become zero.

$$\begin{aligned} J = (\boldsymbol{Y}_R - \boldsymbol{Y}_K)^T R_y (\boldsymbol{Y}_R - \boldsymbol{Y}_K) \\ + \Delta \boldsymbol{U}_{K-1}{}^T R_u \Delta \boldsymbol{U}_{K-1} \end{aligned} \quad (47)$$

$$y = [0\ 0\ 0\ 1\ 0][R, V_R, \lambda, V_\lambda, \gamma_M] \quad (48)$$

The maximum lateral accelratoin of the considered interceptor at sea level is 150 m/s^2. Fig. 4 illustrates acceleration constraint versus altitude. In this study, the maximum lateral acceleration constraint has been considered a function of height. The maximum lateral acceleration is calculated by equation (49) [30].

$$\boldsymbol{a_{z\_max}} = .\boldsymbol{5\rho V_M{}^2 s c_{zmax}/m} \quad (49)$$

the interceptor velocity (V_M), normal force coefficient (c_{zmax}), weight (m), and reference area(s), are considered to be fixed. the maximum acceleration depends on air density which is described by equation 50.

$$a_{z\_max} = \begin{cases} 150.0132\left(\dfrac{287.827}{287.827-0.0065h}\right)^{-4.258} & 0 \le h < 11000 \\ 44.4927e^{\frac{284.0406(11000-h)}{1798616.229}} & 11000 \le h < 25000 \\ 4.8798\left(\dfrac{216.327}{216.327+0.001033*(h-25000)}\right)^{34.0714} & 25000 \le h < 60960 \end{cases} \quad (50)$$

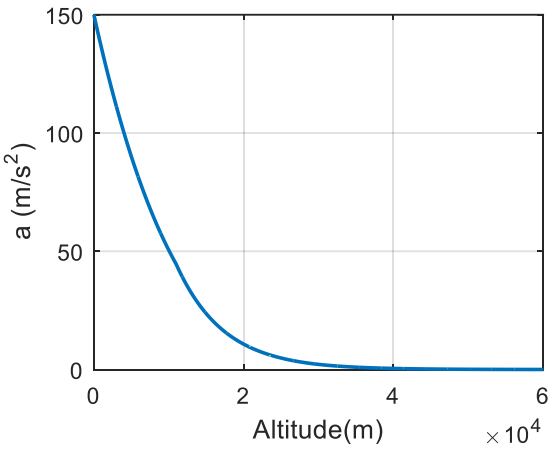

Fig. 4 Acceleration constraint

Numerical simulations are presented to investigate the characteristics and the performance of the proposed guidance law. The results are compared with proportional navigation and sliding mode guidance law with a finite time convergence [8]. In the simulation performed by this reference, the target's velocity is higher than that of the interceptor, and the engagement is head-on.

In this method, the line-of-sight rotation rate turns zero in a finite time. Simulations were performed in a MATLAB environment. Later, we will find that the method proposed in this study zeros the line-of-sight rotation rate faster than the method presented in the reference [8]. The initial position of the interceptor is $xm(0) = 0$, $ym(0) = 0$. Its initial velocity and flight-path angles are Vm = 1200 m/sec and γ_M=90 deg respectively. The initial position of the target is $x_t(0)$ = 100 km and $y_t(0)$ = 500 km. Its initial velocity and flight-path angles are V_t = 3000 m/sec and γ_t = -100 deg respectively. In continuation, the simulation results will be discussed. All the simulation results were carried out using a corei7 processor with a discretion time of 10 msec.

Comparison between the Unconstrained and the Constraint Algorithm

Interceptor accelerations in unconstrained and constraint modes are shown in Fig. 5. In the unconstrained mode, the maximum acceleration is 189 m/sec². As increasing the height decreases the maximum acceleration in a constraint mode. The line-of-sight angle is shown in Fig 6. The changes in this angle converge to zero faster without constraint.

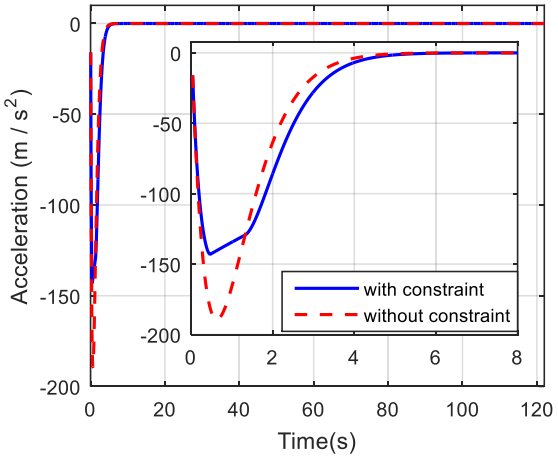

Fig. 5 Acceleration command

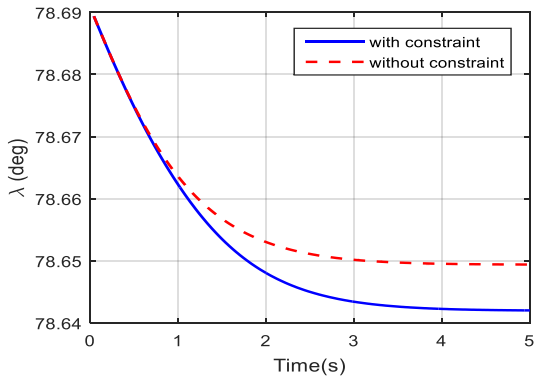

Fig. 6 Los angle

The relative range between the interceptor and the target is shown in Fig. 7. In both methods interceptor acceptably approaches the target.

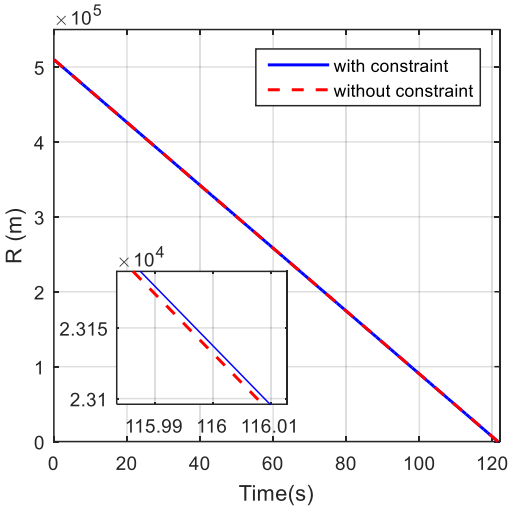

Fig. 7 Relative range

Comparing the Proposed Algorithm with Other Methods

In this section, the performance of the designed guidance through two proportional and sliding mode methods with a finite time convergence [8] is compared.

First, the proposed constraint algorithm is compared with the two other methods with no restriction in the acceleration command. The simulation results for the three guidance laws are shown in Fig. 8-10 The acceleration command is shown in Fig. 8. The acceleration profile plots show that The proposed method produces greater acceleration command at the beginning of guidance than the others. The acceleration command is non-zero until reaching the target in the proportional navigation method; however, the new method acceleration command immediately converges to zero.

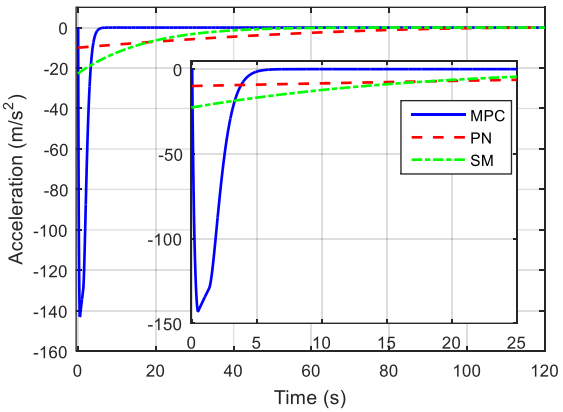

Fig. 8 Acceleration command

The line-of-sight angle and its rate are shown in Figs 9 and 10, respectively. In the proposed method, line-of-sight angle variations converge to zero faster.

The large acceleration of the proposed method at the beginning of the guidance process causes the interceptor to be on the collision course. All three ways acceptably approach the target. The constrained law cannot maneuver in high altitudes; however, this limitation does not exist in others.

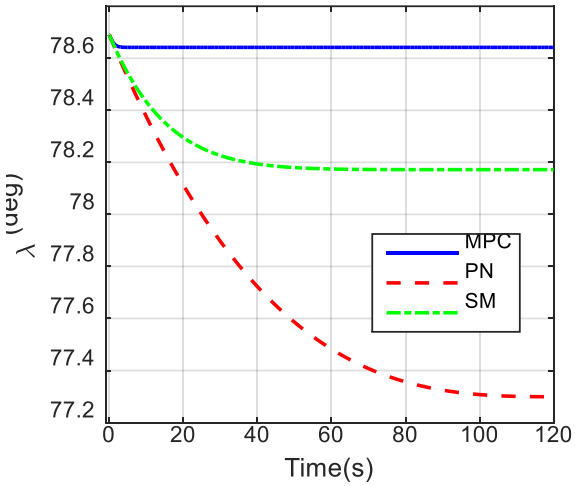

Fig. 9 LOS angle

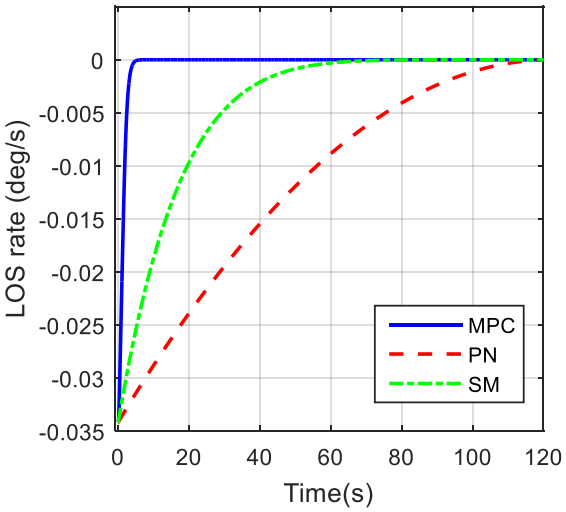

Fig. 10 LOS angular rate

In the second comparison, altitude-dependent acceleration saturation has been considered on the command produced by the other two methods.

The interceptor's acceleration command is shown in Fig. 11. Increasing the height, decreases in atmosphere density, so the interceptor cannot correctly perform the guidance commands. This is quite evident in the performance of proportional

guidance and sliding mode (comparing Figs 11 and 8). Considering the guidance error compensation at the beginning of the process in the proposed method, guidance commands converge to zero after five seconds.

The relative range between the interceptor and target is shown in Fig. 12. The proposed method approaches the target while the others miss it.

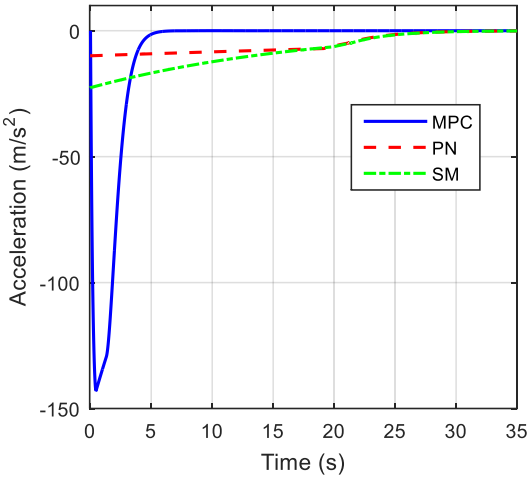

Fig. 11 Actual acceleration

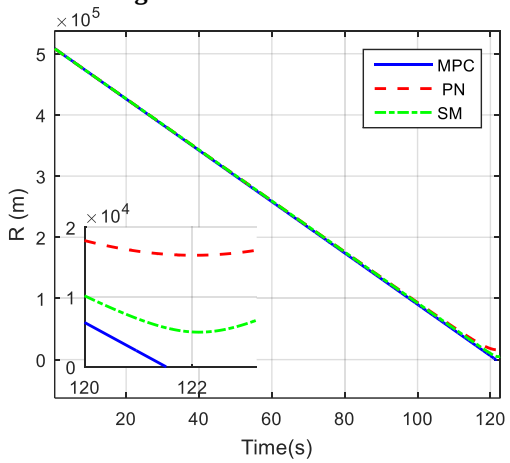

Fig. 12 Relative range

The line-of-sight angle is shown in Fig. 13. The interceptor does not execute the guidance commands in the proportional method and sliding mode due to its height; therefore, the line-of-sight angle changes increase when approaching the target. In the proposed method, the line-of-sight rotation rate turns zero at the beginning of guidance.

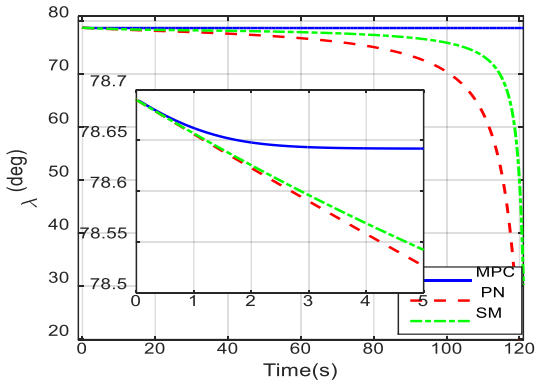

Fig. 13 LOS angle

The interceptor and target position is shown in Fig. 14. The interceptor's course correction at the beginning of guidance is shown in the magnified figure. The proposed method corrects the course at the beginning of the movement.

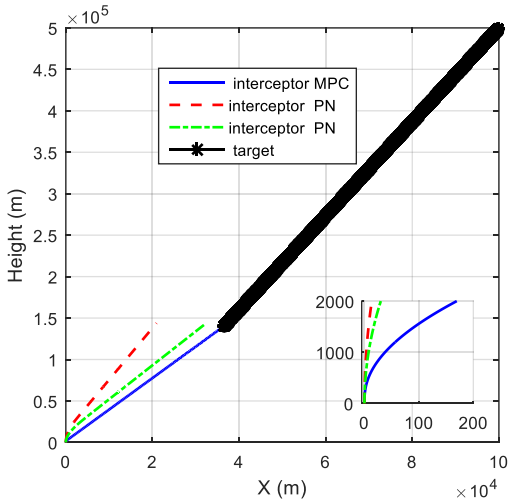

Fig. 14 Trajectories of interceptor and target

Conclusions

This paper proposed a new midcourse guidance method for intercepting high-altitude targets. The proposed method is based on constrained incremental predictive control.

The benefits of the proposed algorithm are:

- at the beginning of the guidance process, a large acceleration command is produced which compensates the guidance error rapidly.
- The system constraints are considered in order to generate the constrained guidance command (maximum acceleration command is a function of interceptor height).
- Simulation results show that the guidance error converges to zero in a finite time. Comparing the proposed method with proportional navigation guidance and sliding mode guidance, it can be

seen that the presented algorithm is more efficient and accurate than the others.

References:

[1] B.-U. Jo and J. Ahn, "Noniterative feedback midcourse guidance for exo-atmospheric interception of ballistic targets using virtual impact point steering," *Aerospace Science and Technology*, vol. 119, p. 107159, 2021.

[2] S. Zhao, W. Chen, L. Yang, and M. Wang, "Optimal midcourse guidance law for the exo-atmospheric interceptor with solid-propellant booster," *Aerospace Science and Technology*, p. 107670, 2022.

[3] S. Ann, S. Lee, Y. Kim, and J. Ahn, "Midcourse guidance for exoatmospheric interception using response surface based trajectory shaping," *IEEE Transactions on Aerospace and Electronic Systems*, vol. 56, pp. 3655-3673, 2020.

[4] Y. Zhang, H. Wu, J. Liu, and Y. Sun, "A blended control strategy for intercepting high-speed target in high altitude ",*Proceedings of the Institution of Mechanical Engineers, Part G: Journal of Aerospace Engineering*, vol. 232, pp. 2263-2285, 2018.

[5]C. Zhu and D. Mu, "Design of head-pursuit guidance law based on sliding mode control," in *IOP Conference Series: Materials Science and Engineering*, 2019, p. 042076.

[6] T. Shima and O. M. Golan, "Head pursuit guidance," *Journal of Guidance, Control, and Dynamics*, vol. 30, pp. 1437-1444, 2007.

[7] T. Shima and O. M. Golan, "Exo-atmospheric guidance of an accelerating interceptor missile," *Journal of the Franklin Institute*, vol. 349, pp. 622-637, 2012.

[8] K.-B. Li, H.-S. Shin, and A. Tsourdos, "Capturability of a sliding-mode guidance law with finite-time convergence," *IEEE Transactions on Aerospace and Electronic Systems*, vol. 56, pp. 2312-2325, 2019.

[9] Q. Ye, C. Liu, and J. Sun, "A backstepping-based guidance law for an exoatmospheric missile with impact angle constraint," *IEEE Transactions on Aerospace and Electronic Systems*, vol. 55, pp. 547-561, 2018.

[10]W. Yu, W. Chen, L. Yang, X. Liu, and H. Zhou, "Optimal terminal guidance for exoatmospheric interception," *Chinese Journal of Aeronautics*, vol. 29, pp. 1052-1064, 2016.

[11] M.-Y. Ryu, C.-H. Lee, and M.-J. Tahk, "Command shaping optimal guidance laws against high-speed incoming targets," *Journal of Guidance, Control, and Dynamics*, vol. 38, pp. 2025-2033, 2015.

[12] K.-B. Li, W.-S. Su, and L. Chen, "Performance analysis of differential geometric guidance law against high-speed target with arbitrarily maneuvering acceleration," *Proceedings of the Institution of Mechanical Engineers, Part G: Journal of Aerospace Engineering*, vol. 233, pp. 3547-3563, 2019.

[13] Y.-S. Jung, J.-I. Lee, C.-H. Lee, and M.-J. Tahk, "A new collision control guidance law based on speed control for kill vehicles," *International Journal of Aeronautical and Space Sciences*, vol. 20, pp. 792-805, 2019.

[14] Y.-W. Kim, M.-G. Seo, and C.-H. Lee, "Investigation on energy-effective guidance-to-collision strategies for exo-atmospheric interceptors," *Aerospace Science and Technology*, vol. 124, p. 107563, 2022.

[15] B. Gaudet, R. Furfaro, and R. Linares, "Reinforcement learning for angle-only intercept guidance of maneuvering targets," *Aerospace Science and Technology*, vol. 99, p. 105746, 2020.

[16] B. Gaudet, R. Furfaro, R. Linares, and A. Scorsoglio, "Reinforcement metalearning for interception of maneuvering exoatmospheric targets with parasitic attitude loop," *Journal of Spacecraft and Rockets*, vol. 58, pp. 386-399, 2021.

[17] E. B. Camacho, C., *Model Predictive Control*: Springer Press, Sevilla, Spain, 1999.

[18] J. A. Rossiter, *Model Based Predictive Control: A Practical Approach*: CRCPress, New York, United States, 2004.

[19] D. Bhattacharjee, A. Chakravarthy, and K. Subbarao, "Nonlinear model predictive control based missile guidance for target interception," in *AIAA Scitech 2020 Forum*, 2020, p. 0865.

[20] U. Eren, A. Prach, B. B. Koçer, S. V. Raković, E. Kayacan, and B. Açıkmeşe, "Model predictive control in aerospace systems: Current state and opportunities," *Journal of Guidance, Control, and Dynamics*, vol. 40, pp. 1541-1566, 2017.

[21] S. He and D. Lin, "Guidance laws based on model predictive control and target manoeuvre estimator," *Transactions of the Institute of Measurement and Control*, vol. 3 ,۸pp. 1509-1519, 2016.

[22] Z. Li, Y. Xia, C.-Y. Su, J. Deng, J. Fu, and W. He, "Missile guidance law based on robust model predictive control using neural-network optimization," *IEEE transactions on neural networks and learning systems*, vol. 26, pp. 180-3.2014.1809

[23] S. Kang, J. Wang, G. Li, J. Shan, and I. R. Petersen, "Optimal cooperative guidance law for salvo attack: An MPC-based consensus perspective," *IEEE Transactions on Aerospace and Electronic Systems*, vol. 54, pp. 2397-2410, 2018.

[24] V .Bachtiar, C. Manzie, and E. C. Kerrigan, "Nonlinear model-predictive integrated missile control and its multiobjective tuning," *Journal of Guidance, Control, and Dynamics*, vol. 40, pp. 2961-2970, 2017.

[25] J. Wang and S. He, "Optimal integral sliding mode guidance law based on generalized model predictive control," *Proceedings of the Institution of Mechanical Engineers, Part I: Journal of Systems and Control Engineering*, vol. 230, pp. 610-621, 2016.

[26] N. O. Ghahramani and F. Towhidkhah, "Constrained incremental predictive controller design for a flexible joint robot," *ISA transactions*, vol. 48, pp. 321-326, 2009.

[27] Y. B. Shtessel, I. A. Shkolnikov, and A. Levant, "Guidance and control of missile interceptor using second-order sliding modes," *IEEE Transactions on Aerospace and Electronic Systems*, vol. 45, pp. 110-124, 2009.

[28] L. Wang, *Model predictive control system design and implementation using MATLAB®*: Springer Science & Business Media, 2009.

[29] D. Q. Mayne, J. B. Rawlings, C. V. Rao, and P .O. Scokaert, "Constrained model predictive control: Stability and optimality," *Automatica*, vol. 36, pp. 789-814, 2000.

[30] W. F. Phillips, *Mechanics of flight*: John Wiley & Sons, 2004.